Laser Photo-Reflectance Characterization of Resonant Nonlinear Electro-Refraction in Thin Semiconductor Films

Will Chism and Jason Cartwright

Xitronix Corporation, 106 East Sixth Street, Ninth Floor, Austin TX, 78701, USA

Abstract:

Photo-reflectance (PR) measurements provide a non-contact means for the precise characterization of semiconductor electronic properties. In this paper, we investigate the use of a laser beam as the probe beam in the PR setup. In this case it is seen the nonlinear refraction is responsible for the amplitude change of the reflected probe field, whereas the phase change is due to nonlinear absorption. The open aperture condition may then be used to eliminate the spatial phase at the detector, thereby isolating the electro-refractive contribution to the PR signal. This greatly simplifies the PR analysis and allows absolute measurements of electro-refraction in thin semiconductor films. We report the application of the laser PR technique to characterize physical strain in thin silicon on silicon-germanium films.

Keywords: Photo-Reflectance, Non-linear refraction, Strained silicon

---

1. Introduction

Modulation spectroscopy has been used extensively to characterize the material properties of semiconductors [1, 2]. Electro-reflectance (ER) in particular has been used extensively to characterize semiconductor band structure and internal electric fields [3-6]. The ER response is due to a tunnel assisted photo-absorption effect at energies near those of semiconductor interband transitions in the presence of an electric field [6, 7]. As shown by Aspnes, in the low field limit the PR response is proportional to $E^2 \times L(\omega)$, where E is the electric field internal to the semiconductor and $L(\omega)$ is a third derivative lineshape function [8]. The physical origin of the response is a resonant third order nonlinearity involving one probe photon

and two DC field quanta [9]. The lineshape function is sharply peaked at semiconductor interband transitions and accounts for the usefulness of ER in the characterization of semiconductor material properties [1].

Photo-reflectance (PR) is a non-contact form of ER, and is therefore ideal for non-destructive testing of semiconductor electronic properties [6]. In PR, a focused pump light beam, typically generated by a laser, is used to induce a periodic variation in the reflectivity of the sample. Due to the need for spectroscopic information, the conventional PR apparatus typically uses a lamp source passed through a monochromator to form the probe beam. The modulated reflectivity is then recorded by phase locked detection of a second probe light beam coincident on the surface of the sample. The small differential reflectivity may generally be written:

$$\Delta R/R = \alpha\Delta n + \beta\Delta k, \quad (1)$$

where $\Delta R/R$ is the normalized change in reflectivity, $\alpha \equiv 1/R \times \partial R/\partial n$ and $\beta \equiv 1/R \times \partial R/\partial k$ are the "Seraphin coefficients," and Δn and Δk are the pump induced changes in the refractive index and the extinction coefficient, respectively [1].

It has recently been remarked that use of a laser probe beam in combination with open aperture detection may eliminate the absorptive contribution to the PR signal, simplifying the PR analysis [10]. This surprising result is generally not true for conventional PR using lamp based probe beams [11]. However, in conventional PR analysis, it is not necessary to independently determine the refractive and absorptive components (the first and second terms in Eqn. (1), respectively) of the PR signal $\Delta R/R$. Rather, a fit to the overall signal is performed using the third derivative functional form given by Aspnes [11]. This fit procedure yields interband transition energies, amplitudes, and widths. Thus, in conventional PR, it is unnecessary to

independently determine Δn and Δk (or α and β). However, due to the required fitting procedure, it is necessary to obtain a spectral continuum, *i.e.*, to scan the wavelength of the probe beam, in order to obtain the desired information.

In this paper we describe the theory of laser beam propagation as it applies to the case of a probe laser beam in a PR setup, and show the nonlinear electro-refractive component of the PR signal may be isolated in certain experimental situations. The inherent suppression of the absorptive part of the nonlinearity allows the laser PR technique to be used in conditions exhibiting substantial absorption, such as the UV. This result further extends to stratified media in commonly encountered situations, greatly simplifying the data analysis. In order to illustrate the measurement of nonlinear refraction in regions of anomalous dispersion in the presence of strong absorptions, we use the technique to characterize strain in ultrathin strained silicon on silicon-germanium films.

2. Theory of Laser Photo-Reflectance

The change in optical constants induced in the sample by the focused pump light beam in a PR system may be written $\Delta n = n_2|E|^2$, $\Delta k = k_2|E|^2$, where n_2 and k_2 are the effective non-linear indices. In PR, the modulation of the sample's internal electric field is due to photo-excited carriers [1,6]. Thus the electro-modulation follows the profile of the pump beam (neglecting diffusion). Assuming a focused pump laser beam traveling in the $+z$ direction, the spatial profile of the induced electro-modulation may be written as:

$$|E|^2 \propto \frac{|E_p|^2}{1+\left(Z/z_p\right)^2}\exp\left\{-\frac{2\rho^2}{\omega_e{}^2(Z)}\right\}, \quad (2)$$

where $|E_p|^2$ is the intensity of the pump beam at focus, Z is the position of the sample with respect to the plane of focus, $z_p = \pi\omega_{po}{}^2/\lambda_p$ is the Rayleigh range of the pump beam, ω_{po} is the

pump beam waist, λ_p is the pump beam wavelength, ρ is the radial coordinate measured from the axis of the pump beam, and $\omega_e(Z)$ is the effective radius of the electro-modulation induced in the sample by the pump beam [12–14]. The effective radius of modulation is ${\omega_e}^2(Z) = {\omega_p}^2(Z) + \mu^2$, where ${\omega_p}^2(Z) = {\omega_{po}}^2\{1+(Z/z_p)^2\}$ and μ is the carrier diffusion length.

Assuming the probe laser beam is collinear and co-focused with the pump beam, the electric field of the reflected probe laser beam at the surface of the sample (disregarding the common spatial phase) is:

$$E_r = \frac{E_0\omega_0}{\omega(Z)}\exp\left\{-\frac{\rho^2}{\omega^2(Z)}\right\}\left[\tilde{r} + \frac{\partial\tilde{r}}{\partial n}(n_2 + ik_2)\frac{|E_p|^2}{1+\left(Z/z_p\right)^2}\exp\left\{-\frac{2\rho^2}{{\omega_e}^2(Z)}\right\}\right], \quad (3)$$

where $|E_o|^2$ is the intensity of the probe beam at focus, ω_o is the probe beam waist, $\omega^2(Z) = {\omega_o}^2\{1+(Z/z_o)^2\}$, $z_o = \pi{\omega_o}^2/\lambda$ is the Rayleigh range of the probe beam, λ is the probe beam wavelength, and $\tilde{r}$ is the complex reflectance coefficient [15, 16]. The first term in Eqn. 3 is the linear portion of the reflected field whereas the second term is the nonlinear contribution.

Writing the standard substrate reflectance coefficient as $\tilde{r} = \frac{n+ik-1}{n+ik+1} = rexp\{i\theta\}$, where r and θ are real, and taking $n^2 \gg k^2$, it is seen $\theta \ll 1$ and $\tilde{r} \cong |\tilde{r}|$. Thus, as shown by Eqn. 3, for reflection from a substrate under the condition $n^2 \gg k^2$, the nonlinear refraction is responsible for the amplitude change of the reflected probe light field, whereas the phase change is due to nonlinear absorption. Many common semiconductors satisfy $n^2 \gg k^2$ from the visible into the near UV [17]. For example, for reflection at 375 nm from a Si substrate, $r \cong 0.74$ and $\theta \cong 0.06$ radians (see Ref. 17). Similarly, $\tilde{r} \cong |\tilde{r}|$ holds for a single thin layer on a substrate where $n^2 \gg k^2$ is satisfied for the top film and an analogous relation $m^2 \gg l^2$, holds for the substrate, in particular:

$$\theta \cong \frac{-r_m(1+r_n^2)\sin\{\frac{4\pi nd}{\lambda}\}}{r_n(1+r_m^2)+r_m(1+r_n^2)\cos\{\frac{4\pi nd}{\lambda}\}}, (4)$$

where $r_n = \frac{n-1}{n+1}$ and $r_m = \frac{m-n}{m+n}\exp\{-\alpha d\}$ are real, d is the overlayer thickness, and $\alpha = 4\pi k/\lambda$ is the overlayer absorption coefficient. Eqn. 4 is applicable to many commonly encountered situations, such as for example, dielectric or semiconductor overlayers on optically thick substrates. As seen, θ approaches zero for small d (vanishing overlayer thickness) or large αd (optically thick overlayer). Furthermore, the phase is limited to $\theta \ll 1$ provided $m \approx n$, which illustrates that the optical phase is additionally limited by a lack of contrast between the refractive indices of the overlayer and substrate. This situation is common whenever the overlayer has a composition similar to the substrate. For example, for reflection at 375 nm from a Si overlayer on a $Si_{0.8}Ge_{0.2}$ substrate, the maximum value of the optical phase is again $\theta_{max} \cong 0.06$ radians.

In such cases the coherent wavefront of the reflected probe laser beam may be integrated at the photo-detector to eliminate the spatial phase shift arising from Δk. In particular, if the reflected probe laser beam is integrated at an aperture, the PR signal may be written:

$$\frac{R+\Delta R}{R} \equiv \frac{\int_0^\infty |E_r|^2 \rho d\rho}{\int_0^\infty |E_{lin}|^2 \rho d\rho}, (5)$$

where E_{lin} refers to the linear portion of the reflectance signal [16, 18]. Performing the integration at the sample surface and taking into account $n_2|E_p|^2 << 1$, $k_2|E_p|^2 << 1$, yields $\Delta R/R \approx 1/r \times \partial r/\partial n \times n_2|E_p|^2/\{1+(Z/z_p)^2\}$. Thus, when the spatially coherent wavefront of the reflected probe laser beam is integrated, the PR signal arises from just the nonlinear electro-refraction and takes the simplified form $\Delta R/R \cong \alpha\Delta n$. A similar result holds for idealized point sources due to

the spherical nature of the light propagation. However, the electro-absorptive contribution cannot be neglected in the standard PR setup due to the spatial extent of the lamp source. Thus, the ability to independently characterize the nonlinear refraction depends upon the coherent phase front of the probe laser beam.

The ability of laser PR to independently characterize nonlinear refraction also extends to stratified media satisfying the condition $\tilde{r} \cong r$ since the electric field of the reflected probe beam at the surface will then contain a series of terms proportional to $\mathrm{Re}[\partial r/\partial n_j \times (\Delta n_j + i\Delta k_j)]$, where j is just the layer index, implying the PR signal may be written: $\Delta R/R \cong \Sigma_j\ \alpha_j \times \Delta n_j$, where $\alpha_j = 1/r \times \partial r/\partial n_j$ are the generalized Seraphin coefficients, and Δn_j are the pump induced changes in the refractive index for each layer [19].

The application of the laser PR technique to resonant nonlinear electro-refraction measurements involves selecting the laser probe beam wavelength very near a strong interband transition. For example, the specific application of the technique to strained silicon measurements requires selection of the laser probe beam wavelength very near the Si E_1 interband transition. In this region, the PR response is highly sensitive to strain due to the third derivative lineshape and due to the shift of the E_1 transition with strain. In particular, the Si E_1 transition is known to undergo a split and shift under strain according to: $E_{1\pm} \cong E_1 + \Delta E_H \pm \Delta E_S$, where ΔE_H (< 0) and ΔE_S correspond to the hydrostatic and shear induced shifts, respectively [20]. Either term is linear in strain. However, the light hole oscillator strengths are typically predominant in the PR spectra of silicon germanium alloys [11, 21–23]. The shift of the light hole transition may be calibrated to the in-plane biaxial tensile strain using the relation: ΔE_{LH} [eV] = -0.1375χ [%], where χ corresponds to the physical strain expressed in percentage strain (absolute) [23]. Near the silicon E_1 interband transition (in the range where $L(\omega)$ exhibits

anomalous dispersion) the PR signal takes the form $\Delta R/R \cong m\chi + b$, where $b=\Delta R/R(0)$ and $m=0.1375\times E^2\times \partial L(\omega)/\partial\omega$. Thus the PR signal is linearly proportional to strain.

3. Experimental Details

In order to illustrate use of the laser PR technique to characterize physical strain in thin semiconductor films, thin Si films were deposited on virtual SiGe substrates. The lattice mismatch between the Si overlayer and the virtual substrate produces a biaxial tensile strain in the overlayer. The virtual SiGe substrates were formed by sequential deposition of four SiGe layers, each of ~500 nm thickness, on a 300 mm Si(100) substrate. The first three layers had nominal Ge compositions of 0.07, 0.13, and 0.19, with the final relaxed SiGe layer having a nominal Ge composition of 0.20. Thin silicon films with thicknesses in the range from 1.5 to17.5 nm were then deposited on the virtual SiGe substrates using low pressure chemical vapor deposition at 700 °C. The thin silicon overlayers were intended to achieve a progression of physical strain values within the top silicon films ranging from maximally strained (pseudomorphic) for the thinner films to fully relaxed for the thicker films. X-ray diffraction (XRD) measurements were performed with a Bede D1 XRD system. Reciprocal space maps were generated from scans using the triple axis diffraction configuration [24]. The lattice spacing in the final SiGe layer was determined to be approximately $0.3a_{Si} + 0.7a_{SiGe}$, where a_{Si} and a_{SiGe} refer to the unstrained lattice constant of Si and $Si_{0.8}Ge_{0.2}$, respectively. Thus, the virtual SiGe substrates exhibit a relative relaxation of approximately 70%. Since a_{Si} is about 1% smaller than a_{SiGe} , the absolute relaxation of the SiGe substrate is ~0.7%. However, the strain in the top Si films could not be resolved using XRD due to the small volume of the Si overlayers.

Due to the inability of XRD to characterize strain in the Si overlayers, reference measurements were performed using UV Raman spectroscopy. UV Raman is generally

preferable to visible Raman for the investigation of strained Si overlayers due to the smaller sampling depth and the resonant enhancement of the Raman signal. The 363.8 nm line of an Ar^+ laser was used as the excitation beam. The UV Raman measurements were carried out through a microscope objective in the back scattering configuration along the [100] direction. In the back scattering geometry used here, only the longitudinal optical (LO) phonon is observed. For the Si on SiGe films the UV Raman spectra were dominated by the signal from the Si overlayer. As is well-known, the Raman shift of the LO phonon in the Si overlayer may be used to estimate strain according to an empirical linear relationship [25]. Thus the nonlinear refraction determined from laser PR is expected to be linearly correlated to the Raman shift.

The basic laser PR setup is shown in Fig. 1. The pump laser is a 488 nm wavelength diode laser operating at approximately 10 mW of power. The pump laser amplitude is modulated using a 1 MHz square wave reference signal from the lock-in amplifier. The modulated pump laser beam is directed at normal incidence onto the sample using a 20X achromatic objective. The spot size is approximately 6 microns, producing a focused intensity $\sim 10^4$ W/cm^2. In undoped Si, this intensity will produce an electrically neutral electron-hole density $\sim 10^{18}$/cm^3 at the surface [26]. As noted, when an electric field is present at or near the surface of the sample, photo-generated carriers will separate and reduce the electric field. In modern ultra shallow junction structures with doping densities $\sim 10^{21}$/cm^3, such a pump intensity only slightly perturbs the junction field [27]. The probe laser is a 374 nm wavelength diode laser operating at approximately 1 mW. The probe laser beam is passed through a beam collimator and a polarizing beam splitting cube (PBC), then combined with the pump beam using a dichroic beamsplitter, and passed through a quarter wave plate (QWP). The collinear pump and probe beams are focused to a common focal point at the sample surface by the achromatic objective.

The beam collimator may be used to precisely adjust the waist of the probe beam to the waist of the pump beam. For SiGe samples such as the samples studied here, the 1 mW probe power is small enough to avoid significant reduction of the near surface electric field due to the carriers generated by the probe [28]. The probe beam is retro-reflected to the PBC, where it is switched out of the incident path due to the polarization rotation induced by the QWP. Any pump light remaining in the reflected probe beam is attenuated using dielectric antireflective mirrors in combination with a color filter. The reflected probe light is collected and integrated at the photodiode. The output photocurrent is passed to the lock-in amplifier, which measures the amplitude and sign of the reflectance change.

Each wafer was located at $Z \cong 0$ using the symmetry of the PR signal about Z. The reflected probe light was collected and integrated at the photodiode. The measurement itself takes approximately one second. Each measurement was repeated 100 times and short term measurement repeatability was determined to be less than less than 5 ppm for each wafer tested. Long term stability was ensured through calibration of the experimental data to measurements on reference samples.

4. Results and Discussion

Fig. 2 shows the experimental laser PR signal (vector) for the strained silicon on silicon germanium films. The trajectory of the PR signal is oriented primarily along a line which may be taken to define the in-phase component of the signal. The out of phase (quadrature) component of PR signal characterizes the time lag of the PR signal and should not be confused with the optical phase. As noted, for the two-layer stack, the PR signal is represented by a sum of two vectors, one describing the refractive component of the PR signal reflected from the overlayer, and a second refractive component of the signal reflected from the substrate. The

exhibited translation of the measured PR signal from its value on the SiGe substrate suggests a large component of the PR signal arising from the overlayer. Once the generalized Seraphin coefficients for each layer are calculated, the PR data shown in Fig. 2 may be used to simply determine Δn (or equivalently, n_2) in the thin silicon film. However, in order to calculate the generalized Seraphin coefficients it is necessary to know the top silicon thickness. The linear reflectance was measured at the pump and probe wavelengths and a regressive fit was performed to determine the physical thicknesses of the sample overlayers. The generalized Seraphin coefficients were then calculated numerically using Si and Ge optical constants from the literature [17]. Over the range of thickness 0-20 nm, the calculated generalized Seraphin coefficients (not shown) are nearly monotonic and do not produce a strong interference effect in the PR data.

To determine the modulated changes of the SiGe substrate dielectric function, the in-phase component of the PR signal on the SiGe "substrate only" sample is divided by the value of the substrate Seraphin coefficient for the substrate. Since 488 nm wavelength light has an absorption depth of 500 nm in silicon, pump induced electro-modulation is approximately constant over the sample set. Then $\Delta R/R \cong \Sigma_j \alpha_j \times \Delta n_j$ is solved for each sample with a Si overlayer using the calculated Seraphin coefficients to weight the electro-refractive response of the overlayer and the substrate.

Fig. 3 shows the derived nonlinear refraction compared with the UV Raman reference measurements and confirms the expected linear correlation between nonlinear refraction and Raman shift (or strain). Taking the position of the Raman peak for the thickest overlayer as the unstrained Si reference value, the strain of the thinnest Si overlayer is seen to be ~0.7%, consistent with value expected from the XRD reference measurements on the SiGe substrate.

In order to determine overlayer strain values from the PR measurements, the linear correlation between the measured n_2 and strain was used. The electro-refractive response of the thickest overlayer was again taken as the unstrained Si reference value, whereas the response thinnest overlayer was taken as the maximally strained (~0.7%) Si reference value (consistent with the XRD and UV Raman reference data). Fig. 4 shows the resultant overlayer strain as a function of overlayer thickness. The data exhibits limiting behavior indicating strain relaxation with increasing overlayer thickness, with essentially complete relaxation beyond a thickness of ~10 nm. In all cases the 1σ precision is less than 3% of the derived value for strain and is typically about 1.5%.

5. Conclusions

The laser PR technique discussed herein has been used for characterization of nonlinear electro-refraction in thin semiconductor films. The laser probe beam provides a coherent wavefront upon reflection from the sample and which may be integrated at the photodetector to independently determine the refractive contribution to the PR signal. The inherent suppression of the absorptive part of the nonlinearity allows this technique to precisely measure n_2 in regions of anomalous dispersion in the presence of strong absorptions. The measured n_2 may be used to determine interband transitions and related physical quantities in thin semiconductor films, such as strain in thin silicon films. Additionally, the use of laser PR combines high measurement speed with long term measurement stability. The simplicity and sensitivity of the laser PR technique make it attractive as a rapid and precise means to characterize the resonant nonlinear refraction of thin semiconductor films.

Acknowledgments

Will Chism wishes to thank Michael Current for useful discussions. The strained silicon samples and XRD reference measurements used in this study were provided by International SEMATECH Manufacturing Initiative, Inc., courtesy of Victor Vartanian. The Raman reference measurements were provided by Wafermasters, Inc., courtesy of Woo Sik Yoo.

References

[1] D. Aspnes, in: M. Balkanski (Ed.), Handbook on Semiconductors, Vol. 2, North-Holland, Amsterdam, 1980, p. 109.

[2] N. Bottka, D.K. Gaskill, R.S. Simon, R. Henry, and R. Glosser, J. Electron. Mater. 17 (1988) 161.

[3] B.O. Seraphin, Phys. Rev. 140 (1965) A1716.

[4] B.O. Seraphin and N. Bottka, Phys. Rev. 145 (1966) 628.

[5] J.S. Kline, F.H. Pollak, and M. Cardona, Helv. Phys. Acta, 41 (1968) 968.

[6] H. Shen and F.H. Pollak, Phys. Rev. B 42 (1990) 7097.

[7] L.V. Keldysh, Sov. Phys.-J. Electron. Theor. Phys. 7 (1958) 788.

[8] D.E Aspnes, Phys. Rev. Lett. 28 (1972) 913.

[9] D.E Aspnes and J.E. Rowe, Phys. Rev. B 5 (1972) 4022.

[10] M. Current, W. Chism, W.S. Yoo, and V. Vartanian, AIP Conf. Proc. 1395 (2011) 165.

[11] R.T. Carline, C. Pickering, T.J.C. Hosea, and D.J. Robbins, Appl. Surf. Sci. 81 (1994) 475.

[12] M. Sheik-bahae, A.A. Said, and E.W. Van Stryland, Opt. Lett. 14 (1989) 955.

[13] M. Sheik-bahae, A.A. Said, T.-H. Wei, D.J. Hagan, and E.W. Van Stryland, IEEE J. Quantum Electron. 26 (1990) 760.

[14] H. Ma and C.B. de Araujo, Appl. Phys. Lett. 66 (1995) 1581.

[15] D.V. Petrov, A.S.L. Gomes, and C.B. de Araujo, Appl. Phys. Lett. 65 (1994) 1067.

[16] D.V. Petrov, J. Opt. Soc. Am. B 13 (1996) 1491.

[17] D.E Aspnes, Phys. Rev. B 27 (1983) 985.

[18] M. Martinelli, L. Gomes, and R.J. Horowicz, Appl. Opt. 39 (2000) 6193.

[19] D.E. Aspnes, J. Opt. Soc. Amer. 63 (1973) 1380.

[20] C. J. Vineis, Phys. Rev. B 71 (2005) 245205.

[21] Y. Yin, F.H. Pollak, P.Auvray, D. Dutartre, R. Pantel, and J.A. Chroboczek, Thin Solid Films 222 (1992) 85.

[22] T.P. Pearsall, in: J.M. Chamberlain, L. Eaves, and J.-C. Portal (Eds.), Electronic Properties of Multilayers and Low-Dimensional Semiconductor Structures, Plenum Press, New York, 1990, p. 375.

[23] H. Chouaib, M.E. Murtagh, V. Guenebaut, S. Ward, P.V. Kelly, M. Kennard, Y.M. Le Vaillant, M.G. Somekh, M.C. Pitter, and S.D. Sharples, Rev. Sci. Instrum. 79 (2008) 103106.

[24] D.K. Bowen and B.K. Tanner, High Resolution X-ray Diffractometry and Topography, Taylor & Francis, London, 1998.

[25] J. Munguia, J.-M. Bluet, H. Chouaib, G. Bremond, and C. Bru-Chevallier, Phys. Status Solidi A 206 (2009) 821-825.

[26] J. Opsal and A. Rosencwaig, Appl. Phys. Lett. 47 (1985) 498.

[27] W. Chism, M. Current, and V. Vartanian, J. Vac. Sci. Technol. B 28 (2010) C1C15.

[28] W. Chism, U.S. Patent Publication No. US 2010/0315646 A1 (2010).

Legends

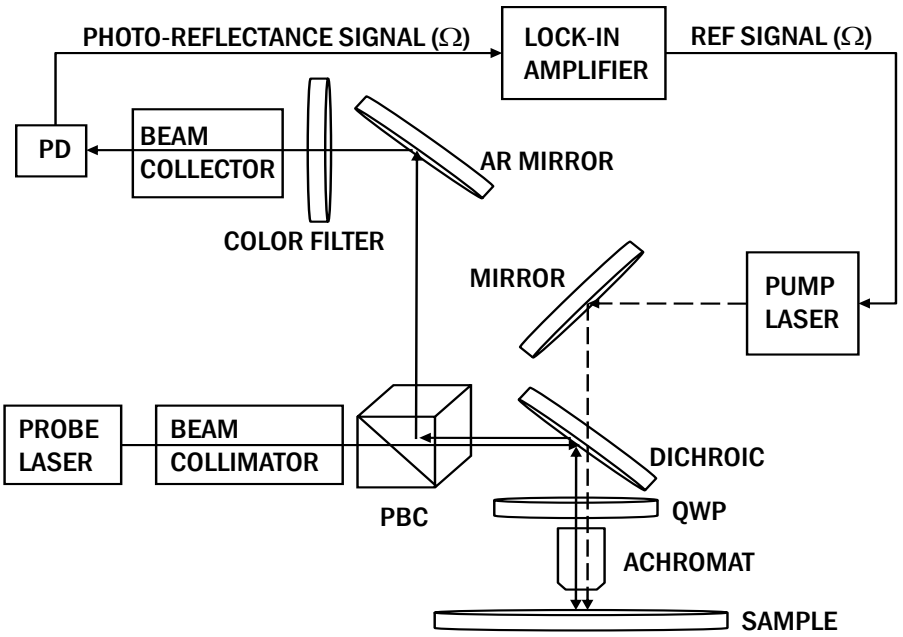

FIGURE 1. Schematic of laser PR apparatus.

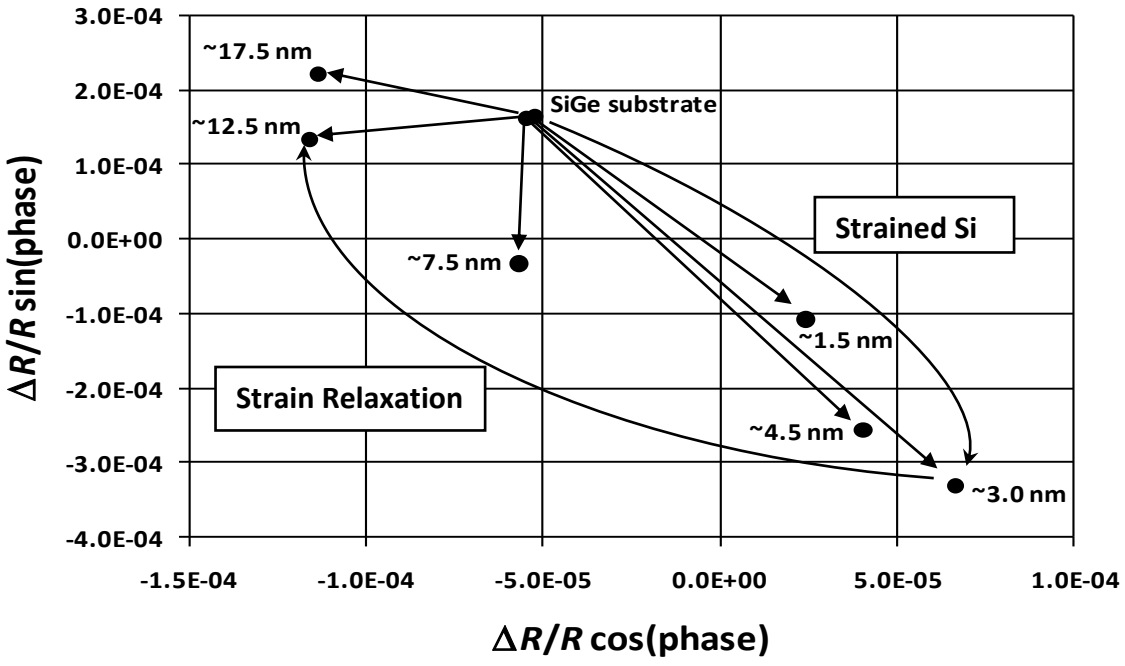

FIGURE 2. Laser PR signal from strained silicon on silicon-germanium substrates (after Ref. 10).

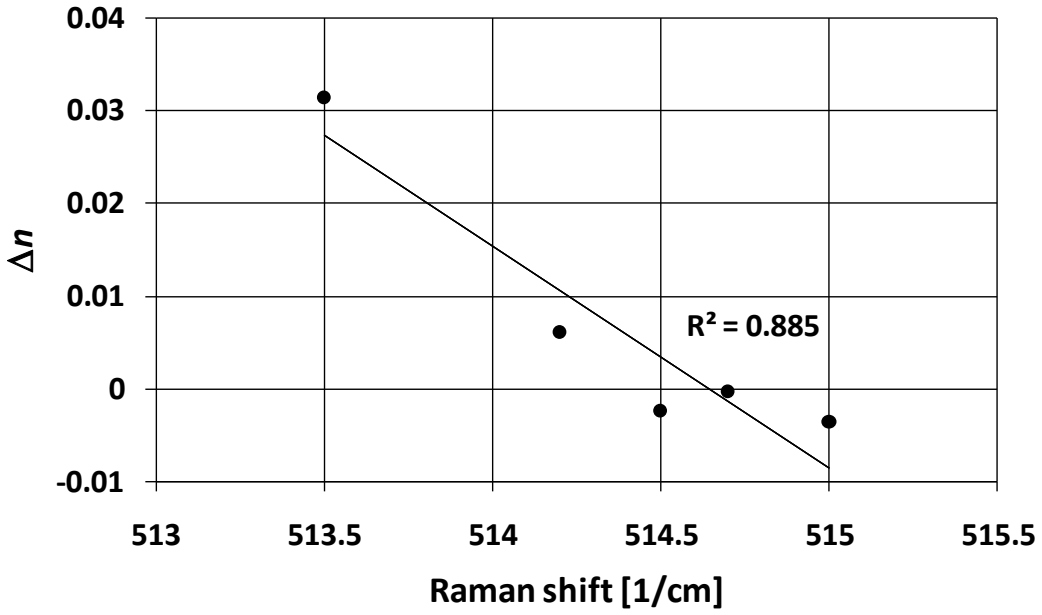

FIGURE 3. Comparison of nonlinear refraction with Raman shift of the LO phonon in Si.

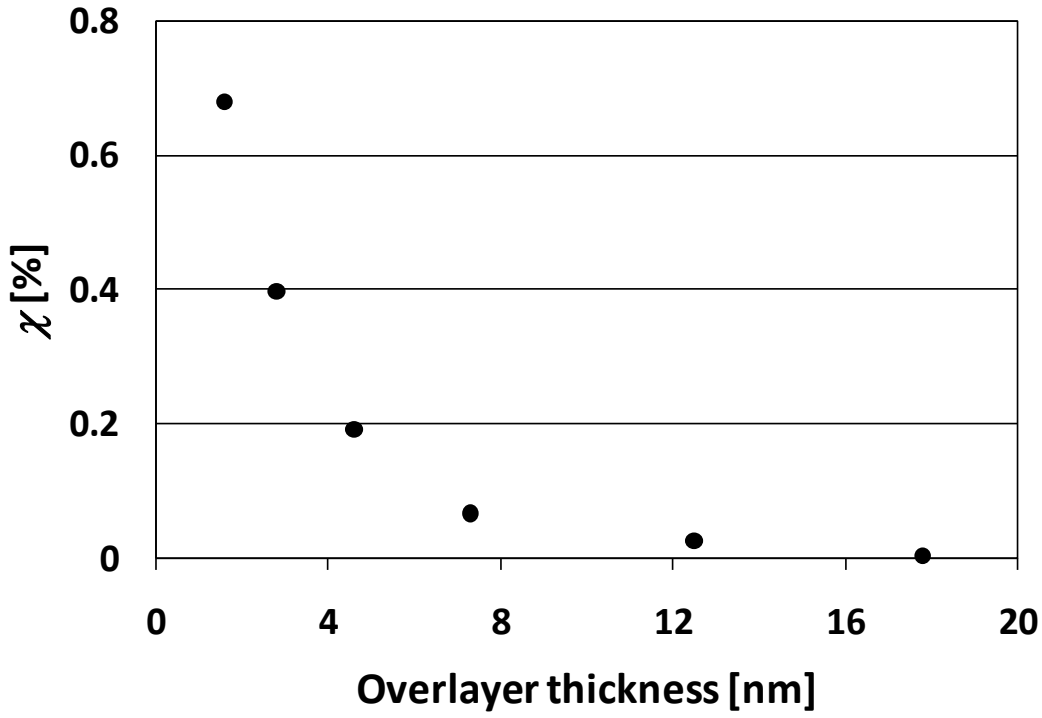

FIGURE 4. Strain in silicon overlayers derived from laser PR measurements.